



大阪

inter-noise 2011

Osaka Japan September 4-7

Real-Time Simulation of Far-Field Rotorcraft Noise with Ground Effects using an Efficient Hybrid Method and GIS

Soogab Lee¹ and Eunkuk Son²

^{1,2}Department of Mechanical and Aerospace engineering, Seoul National University

ABSTRACT

An efficient hybrid method for the prediction of far-field rotorcraft noise with ground effects has been developed. The noise source from rotorcraft is predicted by using a closely coupled aerodynamic and structural methodology and acoustic analogy. Moreover, the ray theory is applied to predict the far-field noise propagation with the effects of ground surface and atmospheric condition. Through this procedure, noise levels near a practical airport region are simulated with GIS (Geographical Information System) terrain profile data.

1. INTRODUCTION

Since a helicopter is on a mission in low altitude and strong unsteady loading is distributed around rotor blades, noise with a high level is propagated on a ground. Residents who live near a heliport or below flight paths have argued on its environmental issues such as cardiovascular diseases, hypotension, sleep disturbance and learning capabilities of their children; therefore, they have strongly demanded that the heliport has to be moved. In this circumstance, reasonable and accurate reference which represents effects on the helicopter noise has been continuously requested; however, it is still on a debate. Mostly recommended material up to now is noise map.

Noise map is well known for a high legibility because each contour expresses different noise level on the ground. Low noise region can be classified when helicopter noise map is used. Also, the flight paths which detour the region of a higher noise level can be designed and barriers can be built in the area below a regular flight path. This useful helicopter noise map can be obtained by means of huge measurements or numerical methods. Although the means of measurements has accumulated a high quality of data and evaluated the region with good accuracy, it consumes a large amount of time and money and is able to assess the only restricted area with unique meteorological data. On the other hand, the latter method can assess any region and simulate a variety of paths with relatively small computation cost. Besides, the variation of noise level by time can be obtained. However, the methods require a high level of numerical technique such as aerodynamic analysis and acoustic source database on the rotor blades and the understanding on sound propagation phenomena in the atmosphere.

In this paper, an efficient hybrid method is applied for the far-field rotorcraft noise. There are two major part of the method. Noise source construction is the first part by using Helicopter Panel Analysis (HeliPA) code based on potential flow. HeliPA is carried out the aerodynamic analysis on the main rotor blades and noise prediction. The latter part of the method is a propagation model based on acoustic ray theory. The propagation model considers the effects of terrain and atmosphere. A diffraction wave caused around the wedge of the obstacle and a refraction wave in a refracting atmosphere can be calculated.

¹ solee@snu.ac.kr

² sonddol@snu.ac.kr

2. Noise prediction on rotor blades

2.1 Aerodynamic analysis

In order to accurately predict aerodynamic noise, most dominant noise sources, of the helicopter, aerodynamic analysis on rotor blades is carried out. It is difficult to analysis without a deformation of blades due to its high aspect ratio and distribution of a high level of unsteady loadings. The finite element method on the first order Euler beam is applied. To consider highly unsteady loading aerodynamic - structure coupled method is used.

The rotor blades are regarded as vortex lattice in the potential fluid flows. Wake is calculated by using the free wake model which calculates wake geometry with time marching. Constant Vorticity contour (CVC) and curved vortex model are also used considering helical tip vortex trajectory.

Each directional mode is calculated after the characteristic equation consisted of stiffness matrix and mass matrix on finite element with the first Euler beam is analyzed. Responses of the blade deformations are calculated with aerodynamic loading, rotating inertia and angular pitch rotation.

Comparison between the results of aerodynamic analysis and baseline condition of HART II is carried out and it is shown as following figure 1 [1]. The experiments are under BVI whose aerodynamic characteristic is extremely difficult to predict.

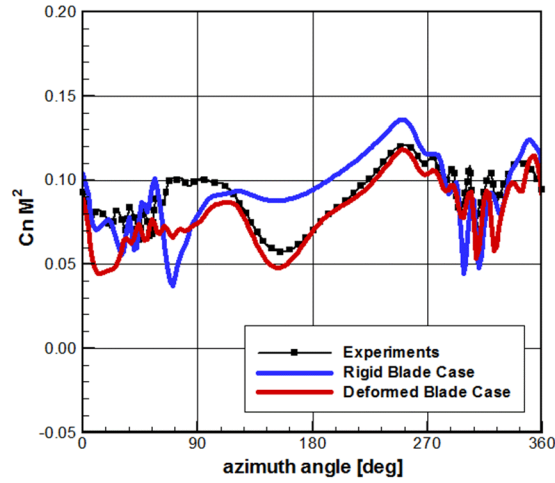


Figure 1 – Azimuthal loading distribution on the rotor blade at $r/R=0.87$

The results represent loading distribution at 87% of blade spanwise by one revolution. The case of deformed blade analysis shows the better agreement with the experiments. It also gives quite good agreement between 270 degree and 360 degree.

2.2 Acoustic analysis

Thickness and loading noise level on the rotor blades are considered by using F. Farassat 1A formula derived from Lighthill's acoustic analogy. Under the subsonic condition, the effects on quadrupole terms are negligible and the equations of thickness and loading noise are as following [2].

$$p'(\vec{x}, t) = p'_T(\vec{x}, t) + p'_L(\vec{x}, t) \quad (1)$$

$$4\pi p'_T(\vec{x}, t) = \int_{f=0} \left[\frac{\rho_0 \dot{v}_n}{r(1-M_r)^2} \right]_{ret} dS + \int_{f=0} \left[\frac{\rho_0 v_n (r\dot{M}_i \hat{r}_i + c_0 M_r - c_0 M^2)}{r^2 (1-M_r)^3} \right]_{ret} dS \quad (2)$$

$$\begin{aligned}
4\pi p'_L(\bar{x}, t) = & \frac{1}{c_0} \int_{f=0} \left[\frac{i \hat{r}_i}{r(1-M_r)^2} \right]_{ret} dS + \int_{f=0} \left[\frac{l_r - l_i M_i}{r^2(1-M_r)^2} \right]_{ret} dS \\
& + \frac{1}{c_0} \int_{f=0} \left[\frac{l_r (r \dot{M}_i \hat{r}_i + c_0 M_r - c_0 M^2)}{r^2(1-M_r)^3} \right]_{ret} dS
\end{aligned} \tag{3}$$

There is also comparison with HART II experiments and numerical results. Acoustic signal is illustrated in figure 2. In figure 2, there is a little difference on the magnitude of acoustic pressure; however, the phase of the peak signal is well predicted. It means that the model has a good capability even in that BVI cases.

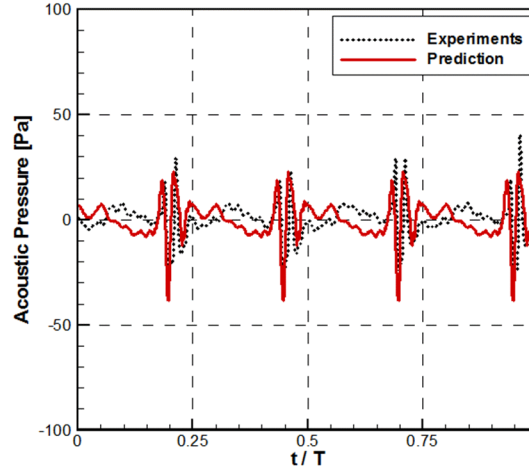


Figure 2 – Comparison on the acoustic signal with HART II experiments

2.3 Noise source database

Acoustic sphere as noise source database can be constructed with function of tip path plane angle and advance ratio. The sphere contains information on the thickness and the loading noise of the main rotor. To avoid the non-linear propagation characteristics in the near field, a radius of the sphere is set over $7R$ [3].

3. Sound propagation

Boundary element method (BEM), parabolic equation (PE) and Acoustic ray theory are most well-known sound propagation model. In real-time simulation of noise, the model should be able to consider complex terrain shape and various environmental parameters in the atmosphere such as temperature variation, humidity and wind speed profile. Acoustic ray model can be satisfied these requirements and simply built.

3.1 Acoustic ray theory

Governing equation of the ray theory is Eikonal equation derived from wave equation with some assumptions. The equation (4) is the Eikonal equation.

$$|\nabla \tau|^2 = \frac{1}{c^2} \tag{4}$$

From the solutions of the equation (4), acoustic ray paths can be known. Noise level with terrain effects and atmospheric effects can be also determined. The equation (5) describes the calculated

noise level at a receiver on the ground by using ray theory.

$$L_R = L_{p_{free}} + \Delta L_{terrain} + \Delta L_{atmosphere} \quad (5)$$

$L_{p_{free}}$ is the sound pressure level on the acoustic sphere's panel. $\Delta L_{terrain}$ represents an attenuation level by the ground reflection or the barrier diffraction. $\Delta L_{atmosphere}$ is the atmospheric effects such as sound absorptions and wave refractions. Finally, L_R is the value at the receiver on the ground [3].

3.2 Terrain effects

Since the receiver is usually located on the ground, sound pressure level (SPL) at the receiver is dependent on terrain shapes and surface. Most surface of the ground is consisted of porous medium whose acoustical characteristics is governed by flow resistivity, a ratio of induced volume flow rate and pressure gradient in unit thickness of the medium. With this ground properties, relative sound pressure level can be determined with impedance calculations.

Wave diffraction occurs when the ray cannot directly arrive from the source to the receiver due to obstacles. The region where the ray cannot be propagated directly is called shadow zone as already well known concept. Though, there are so many models for the calculation on the diffracted wave effects, Salomons' empirical formula which is also applicable in the refracting atmosphere is chosen [4].

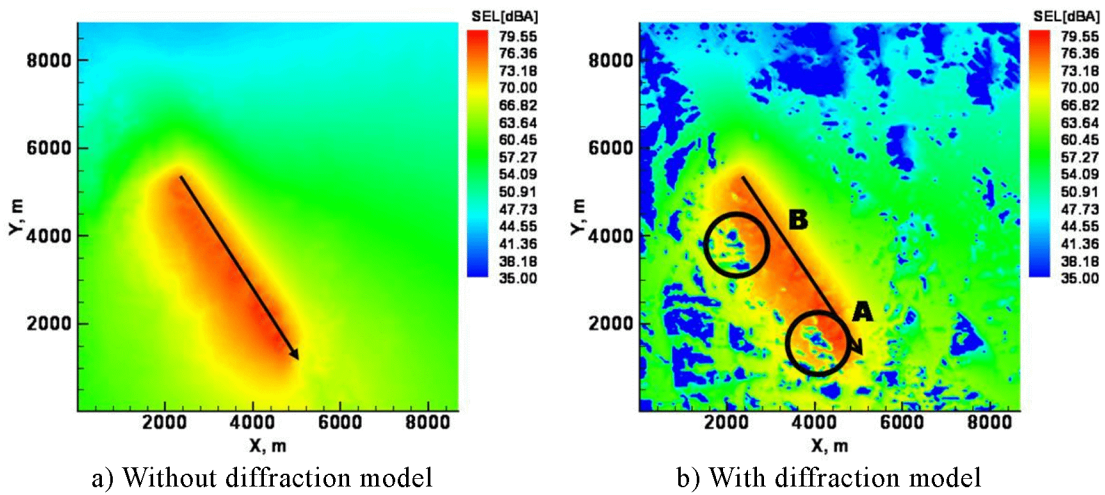


Figure 3 – Diffraction effects in the mountainous area

The black arrow in the figure 3 represents the direction of a helicopter. The terrain height is extracted from GIS. The figure 3 shows average SPL by the event time. Both figure 3-a) and 3-b) show quite different results in the region marked A and B. The ray radiated on the acoustic sphere as mentioned above 2.3 cannot directly propagate to the receiver because of the obstacle, a mountain. Therefore, the ray arrived in the region A and B is diffracted at the edge of the mountain so that the terrain attenuation level is much greater.

3.3 Atmospheric effects

Air absorption is caused by the relative humidity and the interaction between the molecular of the air and by the temperature variation in the atmospheric boundary layer. ISO-9613 fairly describes calculation of the absorption coefficient. Practically, the temperature is not constant and the sound speed in the atmosphere is also not constant. Therefore, mostly the ray cannot directly propagate through the air but it has refracted path. Refracted wave effect is efficiently considered by use the profile of the effective sound speed as follows equation (6).

$$c_{eff} = c_0(z) + u(z) \quad (6)$$

$c_0(z)$ is the sound speed in the adiabatic state and $u(z)$ is the wind speed profile depending on atmospheric stability. The effective sound speed, c_{eff} , is calculated by atmospheric stability parameter, Monin-Obukhov length (L^{-1}). The temperature and wind speed distribution are represented as following equation (7) and (8) with Businger-Dyer relation [5].

$$\bar{\theta}(z) = \theta_0 + \frac{\theta_*}{\kappa} \left[\ln \frac{z}{z_0} - \Psi_t \right] \quad (7)$$

$$\bar{u}(z) = \frac{u_*}{\kappa} \left[\ln \frac{z}{z_0} - \Psi_w \right] \quad (8)$$

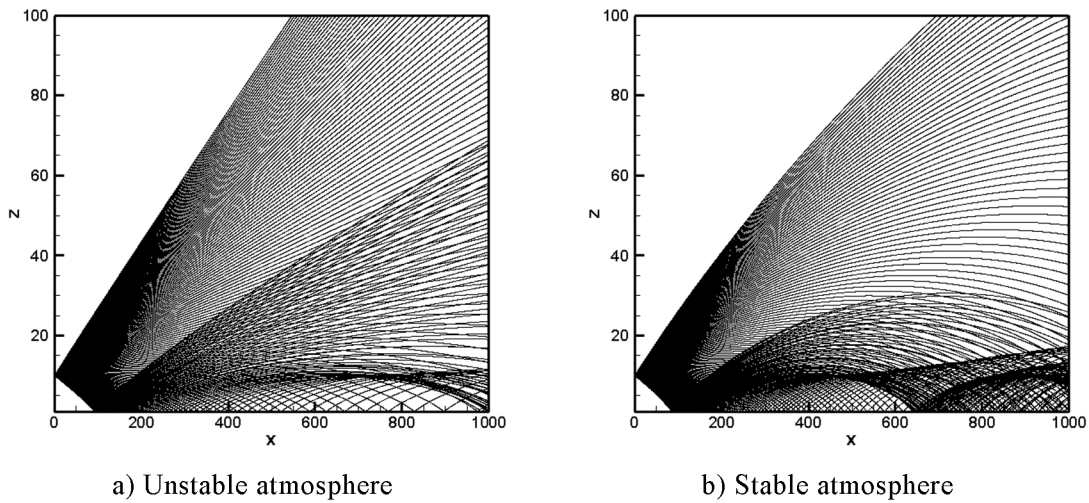


Figure 4 – Ray paths in a refracting atmosphere

The figure 4 shows the results of ray paths both in unstable and stable conditions. In the stable atmosphere, most of rays are refracted downward and there are also multiple reflections. Therefore, in the stable atmosphere, the more number of rays are arrived at the receiver so that these cause a higher noise level than in the unstable atmosphere.

3.4 Geographic information system

To reflect the real terrain in numerical simulations, the model should contain the algorithm which transforms from GIS data to the numerical grid system. Since GIS file contains many kinds of information, the algorithm only extracts necessary data for the simulation. A fine grid system can be obtained after the data extraction by Delaunay Tessellation.

4. CONCLUSIONS

Using GIS data, real-time noise prediction model on a helicopter flight has been developed. GIS data is transformed into the numerical grid system by using Delaunay Tessellation. Aerodynamic loading on main rotor blades is analyzed by HeliPA code based on potential flow. The results of aerodynamic analysis are used for the noise prediction as an input data. F. Farassat 1A formula derived from Lighthill's acoustic analogy is used for the prediction of thickness and loading noise on the main rotor. The thickness and loading noise of the main rotor are to be the database, called 'acoustic sphere'. The database is constructed as function of the tip path plane angle and the advance ratio. With the noise database, the propagation model based on the acoustic ray theory is used and it considers the effects of terrain and atmosphere. Especially, since there is different sound speed profile during the day and the night, the model considering atmospheric stability is applied.

Figure 5 shows the noise map at specific time during the flight of UH-60.

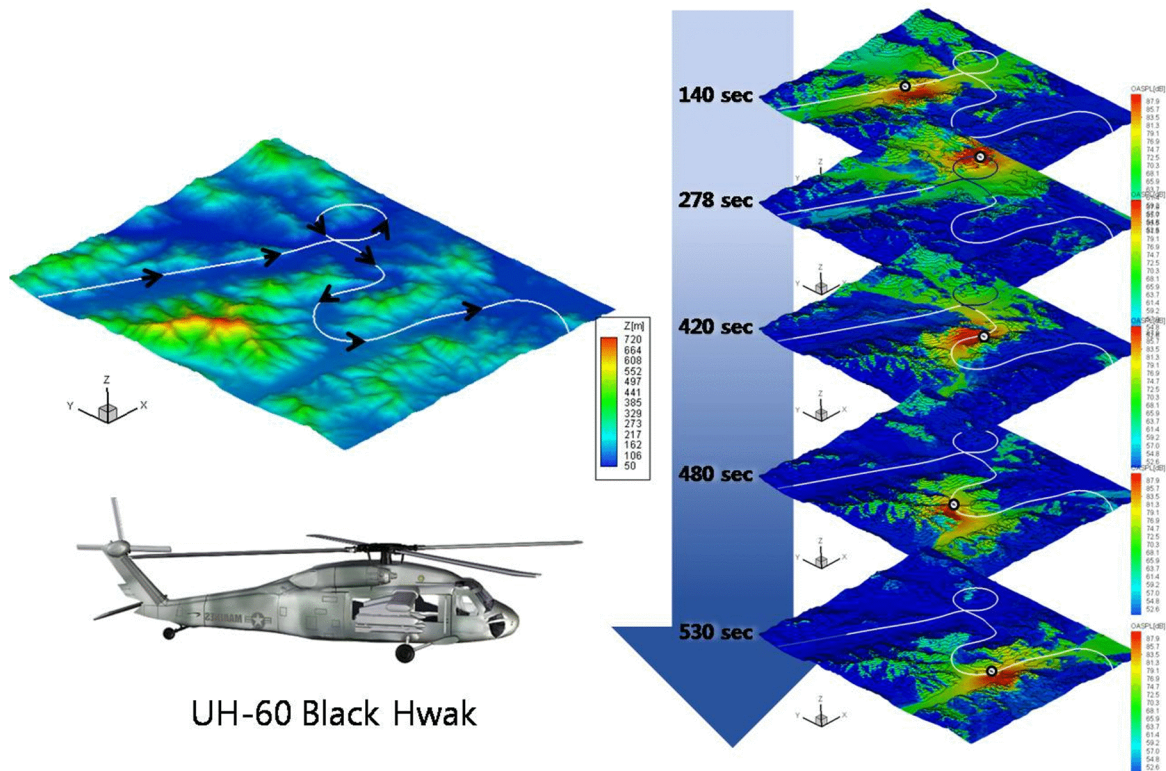


Figure 5 – Real-time noise simulation with GIS

Once noise source database is constructed by using numerical methods as mentioned previously, the noise map on the specific region in real time can be achieved. The results are quite legibility even for common people who may insist that a heliport or an airport must be moved. The helicopter noise map in real-time will be the preferable reference which is able to assess the environmental impacts on the rotorcraft noise near the region of the flight path.

ACKNOWLEDGEMENTS

This work was supported by the Human Resources Development of the Korea Institute of Energy Technology Evaluation and Planning (KETEP) grant funded by the Korea government Ministry of Knowledge Economy (No. 20094020100060) and also supported by the New and Renewable Energy of the Korea Institute of Energy Technology Evaluation and Planning (KETEP) grant funded by the Korea government Ministry of Knowledge Economy (No.20104010100490)

REFERENCES

- [1] Yu, Y. H., Tung, C., van der Wall, B. G., Pausder, H., Burley, C. L., Brooks, T., Beaumier, P., Delrieux, Y., Mercher, E., Pengel, K., "The HART-II Test: Rotor Wakes and Aeroacoustics with Higher Harmonic Pitch Control (HHC) Inputs - The joint German/French/Dutch/US Project," AHS 58th Annual Forum, Montreal, Canada, 2002.
- [2] Z. F. Farassat, "Theory of Noise Generation from Moving Bodies with an Application to Helicopter Rotors," NASA TR R-451, 1975.
- [3] Eunkuk Son, Seungmin Lee, Soogab Lee, "Helicopter noise propagation characteristics in the refracting atmospheric conditions", 20th International Congress on Acoustics, 23-27 August, 2010
- [4] Erik M. Salomons, "Noise Barriers in a Refracting Atmosphere", Applied Acoustics, 1996
- [5] J.A. Businger, J.C. Wyngaard, Y. Izumi, and E.F. Bradley, "Flux-Profile Relationships in the Atmospheric Surface Layer", J. Atmos. Sci. 28, 1971